COBEM 99
XV Congresso Brasileiro de Engenharia Mecânica
15th Brazilian Congress of Mechanical Engineering
22 - 26 de Novembro de 1999 / November 22 - 26, 1999 Águas de Lindóia, São Paulo,

EXPERIMENTAL NEURAL CONTROL OF AN UNCONSTRAINED MULTIBODY SYSTEM WITH FLEXIBLE APPENDAGES

Wilson Rios Neto[1]
Luiz Carlos Sandoval Góes[1]
Cairo Lúcio Nascimento Júnior[2]
[1]Divisão de Engenharia Mecânica-Aeronáutica - IEM
[2]Divisão de Engenharia Eletrônica - IEE
Instituto Tecnológico de Aeronáutica - ITA
12228-900 - São José dos Campos - SP, Brazil
E-mails: wilson@mec.ita.cta.br, goes@mec.ita.cta.br, cairo@ita.cta.br

Abstract. *This paper presents the implementation of an experimental neural control of an unconstrained nonlinear multibody system with flexible appendages, where the appendage-to-hub inertia ratio is 37. The adaptive inverse neural control approach used is called Feedback-Error-Learning and it is based on the use of the output of a feedback controller with fixed parameters to adapt a neural network which acts as a feedforward controller. Firstly the analytical model of the experimental apparatus available at the ITA-IEMP Dynamics Laboratory is derived. The experimental results for the control of this apparatus when using a PID controller and the Feedback-Error-Learning approach are then presented and compared.*

Keywords: *Control of flexible structures, Feedback-error-learning, Nonlinear analytical model, Neural networks.*

1. INTRODUCTION

An important area of research with a great impact in aerospace applications and robotics is the dynamical modeling and control of flexible structures. Presenting a coupling between rigid and flexible motions, flexible structures generally have components with low mechanical rigidity, large number of vibrational modes and low structural damping.

In this article analytical techniques are used to derive the integro-differential equations that describe the motion of the experimental flexible structure available at the ITA-IEMP Dynamics Laboratory. The assumed modes technique is then used to discretize such equations, and as a result a finite-dimensional system of ordinary differential equations is obtained. In this system we are concerned with the natural unconstrained mode of vibration, which is a result of the natural motion of the structure without external influences, i.e., all the structure is allowed to vibrate. In order to find this unconstrained mode of vibration, the inertia and stiffness of the flexible parts have to be considered.

Based on their inherent learning ability and in their massively parallel architecture, artificial neural networks are considered promising controller candidates of nonlinear and uncertain systems. These characteristics have motivated intensive research towards the development of neural network control of flexible structures.

In this article the neural adaptive control approach *Feedback-Error-Learning* (Rios-Neto *et al.*, 1998) is used to control the experimental flexible structure available at the ITA-IEMP Dynamics Laboratory. A PID controller is also used and the experimental results of both strategies are compared.

2. THE ANALYTICAL MODEL FOR THE UNCONSTRAINED MULTIBODY SYSTEM

A schematic view of the experimental setup is shown in figure 1 below. The unconstrained system under consideration is composed of two flexible appendages attached to a rigid hub and driven by a brushless DC motor. The instrumentation system is formed by a tachometer and a potentiometer which measure the hub angular velocity and position, respectively.

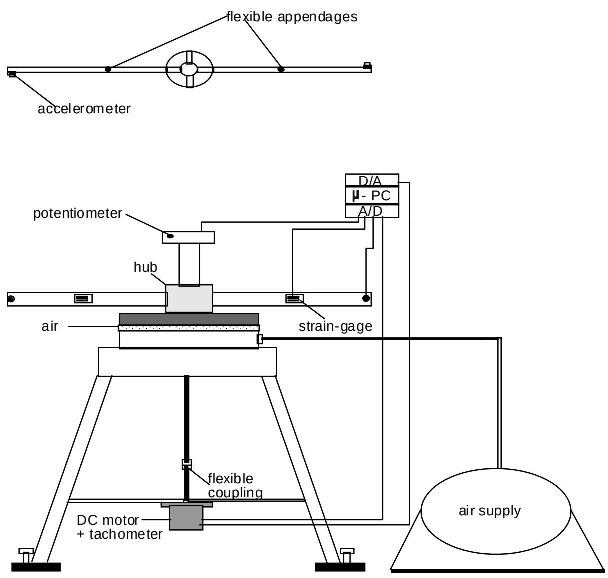

Figure 1- Experimental setup

The Hamilton's principle has been used to determine the differential equations and the boundary conditions for this hybrid system, according to the Lagragian expression: (Barbieri *et al.*, 1988)

$$L = \int_{\Omega} \hat{L}\, d\Omega + L_B \tag{1}$$

where:

$$\hat{L} = \frac{1}{2}\rho\, \dot{\vec{R}}(x)\dot{\vec{R}}(x) - \frac{1}{2} E I\, y''^{2} \tag{2}$$

$$L_b = \frac{1}{2} m_t\, \dot{\vec{R}}(l)\dot{\vec{R}}(l) + \frac{1}{2} I_c \left(\dot{\theta} + \dot{y}'(0)\right) \tag{3}$$

where I_c is the inertia of the hub, ρ is the mass per unit of length of one of the flexible appendage, l is the length of the appendage, m_t the mass of the accelerometer at the tip of the flexible link and the line (') and dot ( ) denote partial derivative with respect to space and time, respectively. Combining eqs. (2), (3) in eq. (1), results:

$$\begin{aligned} L = &\frac{1}{2}\rho\int_0^l (r+x)^2 dx\dot{\theta}^2 + \rho\int_0^l (r+x)\dot{y}dx\dot{\theta} + \frac{1}{2}\rho\int_0^l \dot{y}^2 dx + \frac{1}{2}\rho\int_0^l y^2 dx\dot{\theta}^2 \\ &-\frac{1}{2}\int_0^l EIy''^2 dx + \frac{1}{2}m_t(r+l)^2\dot{\theta}^2 + m_t(r+l)\dot{y}(l)\dot{\theta} + \frac{1}{2}m_t\dot{y}^2(l) \\ &+\frac{1}{2}m_t y^2(l)\dot{\theta}^2 + \frac{1}{2}I_c\dot{\theta}^2 + I_c\dot{\theta}\,\dot{y}'(0) + \frac{1}{2}I_c\dot{y}'^2(0) \end{aligned} \tag{4}$$

Using the generalized Lagrange equation with, $q = [\theta]$, $Q = [\tau]$, the rigid body equation of the system will be given by:

$$\begin{aligned} &\left(\rho\int_0^l (r+x)^2 dx + \rho\int_0^l y^2 dx + m_t(r+l)^2 + m_t y^2(l) + I_c\right)\ddot{\theta} \\ &+\left(\rho\int_0^l (r+x)\ddot{y}dx + m_t(r+l)\ddot{y}(l) + I_c\ddot{y}'(0)\right) \\ &+2\left(\rho\int_0^l \dot{y}dx + m_t\dot{y}(l)\right)y(l)\dot{\theta} = \tau \end{aligned} \tag{5}$$

The elastic equation of the system is, where $y(x,t)$ is the elastic displacement of the beam:

$$\rho\left((r+x)\ddot{\theta} + \ddot{y} - y\dot{\theta}^2\right) + EIy'''' = 0 \tag{6}$$

with the following boundary conditions for a clamped-free system:

$$y(0) = 0 \tag{7}$$

$$y'(0) = 0 \tag{8}$$

$$E\,I\,y''(\mathrm{l}) = 0 \tag{9}$$

$$E\,I\;\; y'''(\mathrm{l}) = m_t\,(\,\ddot{y}(\mathrm{l}) + (\mathrm{l}+r)\ddot{\theta}\,\,) - m_t y(l)\dot{\theta}^2 \tag{10}$$

and, as in Gildin (1997), the momentum balance of the hub is:

$$EI\;y''(0) = I_c(\ddot{\theta} + \ddot{y}'(0)) - \tau_m \tag{11}$$

Introducing a new dependent variable, $z(x,t) = y(x,t) + (x+r)\theta(t)$, the unconstrained mode shape $\phi(x)$ can be found (Rios-Neto, 1998). Thus, the linearized eqs. (5)-(11) are:

$$\rho\ddot{z} + EIz^{iv} = 0 \tag{12}$$

$$I_c\ddot{z}'(0) + \rho\int_0^L (x+r)\ddot{z}dx + m_t(l+r)\ddot{z}(l) = \tau \tag{13}$$

and the following boundary conditions:

$$z(0)=0 \tag{14}$$
$$z'(0)=\theta \tag{15}$$
$$EIz''(l)=0 \tag{16}$$
$$EIz'''(l)-m_t\ddot{z}(l)=0 \tag{17}$$

The momentum balance of the hub is given by $EIz''(0)-I_c\ddot{z}'(0)+\tau=0$. Using: $\theta(t)=\theta\cos(\omega t)$ and $z(x,t)=\phi(x)\cos(\omega t)$, where $\theta(t)$ is the modal amplitudes of the rigid movement of the appendages and $\phi(x)$ the unconstrained modal shapes; in eq. (12) one finds:

$$EI\phi^{iv}=\rho\phi\omega^2 \tag{18}$$

where: $\phi^{iv}=\dfrac{\rho\omega^2}{EI}\phi$ and $\lambda^4=\dfrac{\rho\omega^2}{EI}$.

The above problem admits as a solution the following unconstrained mode shape function:

$$\phi(x)=A\operatorname{sen}(\lambda x)+B\cos(\lambda x)+C\operatorname{senh}(\lambda x)+D\cosh(\lambda x) \tag{19}$$

The constants A, B, C and D are determined from the boundary conditions and a chosen normalization. Evaluating the boundary conditions in eq. (19), we obtain a set of homogeneous equations. For a nontrivial solution, the determinant of the coefficients must vanish, giving the following characteristics equation and unconstrained mode shape function:

$$\begin{aligned}&\frac{2}{I_c\lambda^3}\left[I_c\lambda^6(-1-\cos(\lambda l)\cosh(\lambda l))+(\gamma\lambda l\rho-\lambda^5 lm_t)sin(\lambda l)\right.\\&+(\gamma I_c\lambda^3-\lambda^3\rho)\cosh(\lambda l)\operatorname{sen}(\lambda l)+(l\lambda^5m_t+\gamma l\lambda\rho)\operatorname{senh}(\lambda l)\\&\left.+(\lambda^3\rho-\gamma I_c\lambda^3)\cos(\lambda l)sinh(\lambda l)-2\gamma\rho\operatorname{sen}(\lambda l)\operatorname{senh}(\lambda l)\right]=0\end{aligned} \tag{20}$$

$$\begin{aligned}&\phi(x)=\\&-(D\cos(\lambda x))+D\cosh(\lambda x)+\left(D\operatorname{sen}(\lambda x)l\lambda\rho+I_c\lambda^3\cos(\lambda l)+I_c\lambda^3\cosh(\lambda l)\right.\\&\left.+l\lambda\rho\cos(\lambda l)\cosh(\lambda l)-2\rho sinh(\lambda l)+2l\lambda^2m_t\cos(\lambda l)\operatorname{senh}(\lambda l)+l\lambda\rho\operatorname{sen}(\lambda l)\operatorname{senh}(\lambda l)\right)\\&/\left(\lambda\left(I_c\lambda^2\operatorname{sen}(\lambda l)+l\rho\cosh(\lambda l)\operatorname{sen}(\lambda l)+I_c\lambda^2\operatorname{senh}(\lambda l)-l\rho\cos(\lambda l)\operatorname{senh}(\lambda l)\right.\right.\\&\left.\left.+2l\lambda m_t\operatorname{sen}(\lambda l)\operatorname{senh}(\lambda l)\right)\right)+\left(D\left(l\lambda\rho-I_c\lambda^3\cos(\lambda l)-I_c\lambda^3\cosh(\lambda l)+l\lambda\rho\cos(\lambda l)\cosh(\lambda l)\right.\right.\\&\left.\left.-2\rho\operatorname{sen}(\lambda l)-2l\lambda^2m_t\cosh(\lambda l)\operatorname{sen}(\lambda l)-l\lambda\rho\operatorname{sen}(\lambda l)\operatorname{senh}(\lambda l)\operatorname{senh}(\lambda x)\right)\right)/\left(\lambda\left(I_c\lambda^2\operatorname{senh}(\lambda l)\right.\right.\\&\left.\left.+I_c\lambda^2\operatorname{sen}(\lambda l)I_c\rho\cosh(\lambda l)(\lambda l)\operatorname{sen}(\lambda l)-l\rho\cos(\lambda l)\operatorname{senh}(\lambda l)+2l\lambda m_t\operatorname{sen}(\lambda l)\operatorname{senh}(\lambda l)\right)\right)\end{aligned} \tag{21}$$

where: $\gamma=\dfrac{m_t\omega^2}{EI}$

Using the following orthogonality relationships: (Góes *et al.*, 1998)

$$EI\int_0^l \phi_r''\phi_s''dx = \omega_r^2\delta_{rs} \tag{22}$$

$$\rho\int_0^l \phi_r\phi_s dx + I_c\phi_r'(0)\phi_s'(0) + m_t\phi_r(l)\phi_s(l) = \delta_{rs} \tag{23}$$

The discrete model of the system is obtained by Ritz's Assumed Modes Method. In this method the elastic displacement $y(x,t)$ can be described as:

$$y(x,t) = \sum_{j=1}^{N}\Phi_j(x)\eta_j(t) \tag{24}$$

where $\theta(t) = \sum_{j=1}^{N}\theta\eta_j(t) + \Theta(t)$ and $\Phi(x) = \phi(x) - (x+r)\theta$, with θ as the modal amplitude of the movement; $\phi(x)$ is the unconstrained shape function as demonstrate before and $\Theta(t)$ the rigid body movement of the appendage.

Applying Lagrange method in equations (5) and (6) and using the orthogonality relationships, the following matrix equation is obtained for the modes:

$$M\ddot{q} + D\dot{q} + Kq = F \tag{25}$$

$$M = \begin{bmatrix} \rho\int_0^l (r+x)^2 dx + m_t(r+l)^2 + I_c + \eta^T[MS]\eta & \rho\int_0^l (r+x)\phi^T(x)dx + m_t(r+l)\phi^T(l) + I_c\phi'^T(0) \\ & +\eta^T[MS]\eta\theta^T \\ [\mu s]_T & [MS] + [\mu s]^T\theta^T + I_c(\phi'(0) - r\theta') \\ & (\phi'(0) - r\theta')^T \end{bmatrix} \tag{26}$$

$$D = \begin{bmatrix} 2\dot{\eta}^T[MS]\eta & 2\dot{\eta}^T[MS]\eta\theta^T \\ 0 & 0 \end{bmatrix} \tag{27}$$

$$K = \begin{bmatrix} 0 & 0 \\ 0 & \omega^2 - [MS]\dot{\Theta}^2 - 2\dot{\Theta}[MS]\theta^T\dot{\eta} - [MS]\dot{\eta}^T[\theta\theta^T]\dot{\eta} \end{bmatrix} \tag{28}$$

$$F = [\tau \;\vdots\; 0]^T \tag{29}$$

$$q = [\Theta \;\vdots\; \eta]^T \tag{30}$$

where:

$$[MS] = \left[\rho\int_0^l \Phi\Phi^T dx + m_t\Phi(l)\Phi^T(l)\right] \tag{31}$$

$$\left[\rho\int_0^l (\phi(x) - (x+r)\theta)(\phi(x) - (x+r)\theta)^T dx + m_t(\phi(l) - (l+r)\theta)(\phi(l) - (l+r)\theta)^T\right] \tag{32}$$

$$[\mu s] = \left[\rho\int_0^l (r+x)\Phi^t dx + m_t(r+l)\Phi^t(l) + I_c\Phi'^T(0)\right] \tag{33}$$

$$\left[\rho\int_0^l (r+x)(\phi(x) - (x+r)\theta)^T dx + m_t(r+l)(\phi(l) - (l+r)\theta)^T + I_c(\phi'(0) - r\theta')^T\right] \tag{34}$$

$$\theta = \phi'(0) \tag{35}$$

3. THE FEEDBACK-ERROR-LEARNING APPROACH

The goal of the feedback-error-learning approach is to adjust the parameters (weights) of a neural network (this is called "training the neural network") such that it will be a close approximation of the delayed inverse dynamic model of the system under control (Nascimento Jr., 1994).

In this strategy, a combination of feedback and feedforward controllers are used. The parameters of the feedback controller are fixed during the training of the neural network and adjusted before learning begins, such that, when only the feedback controller is used it stabilizes the system under control.

The neural network is used as a feedforward controller (figure 2) and its weights are adjusted in order to minimize the output of the feedback controller. The neural network weights are initialized such that the output of the network is zero for any input. Therefore, when training begins, the control action is performed just by the feedback controller. As the training progress, the neural network slowly takes over, assuming at the end of the training session most of the control action.

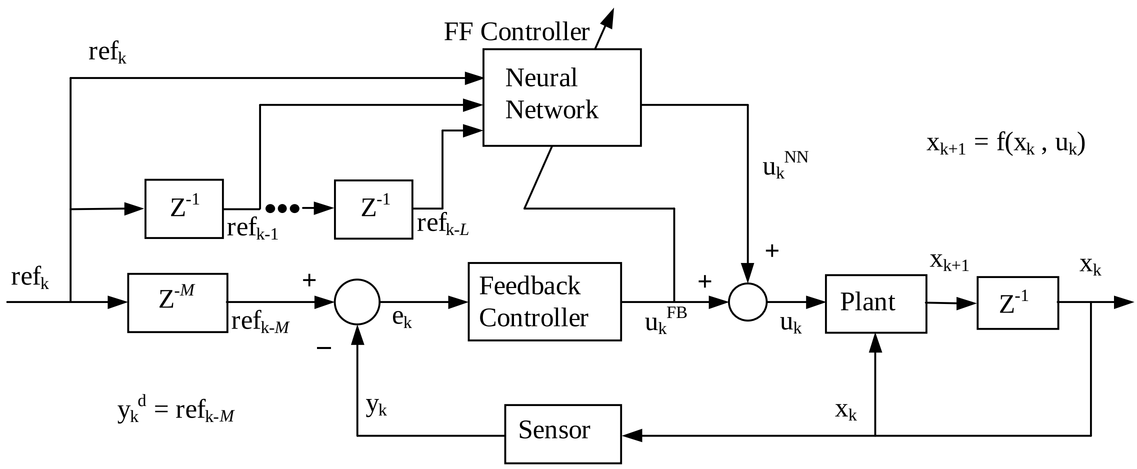

Figure 2- The adaptive inverse control approach *Feedback-Error-Learning*

In Nascimento Jr. (1994), the feedback-error-learning approach was applied to the control of a nonlinear plant using a multilayer Perceptron neural network and the *Feedback-Error-Learning* rule is generalized to the *Back-Propagation* algorithm.

4. EXPERIMENTAL RESULTS

A computer control of the nonlinear unconstrained multibody system with position feedback was setup at the ITA-IEMP Dynamics Laboratory. The objective of this implementation is to compare the performances of a classical *PID* digital controller and the *Feedback-Error-Learning* control approach.

For the multibody flexible system under consideration, the appendage-to-hub inertia ratio is 37. This fact has an impact in the stability of the system and in the implementation of the control approach. It has been shown experimentally that the stability of the system is assured only if the reference signal has low frequencies and low amplitude (Rios-Neto, 1998).

Having in mind that the system under control is nonlinear, a nonlinear neural network model (a multilayer Perceptron with three layers: input/hidden/output) was used as the feedforward controller. The hidden and output network layers used hyperbolic tangent and linear functions respectively. The Back-Propagation algorithm was used to train the neural network during the real-time control experiment. Table 1 below presents the parameters used during the experiment, where K_p, K_i, K_d are the feedback controller parameters, L_{input} and L_{hidden} are the number of units in the input and hidden network layers, η_{input} and η_{input} are the learning rate parameters used by the Back-Propagation algorithm, and M the desired delay for the inverse model of the system.

Table 1. Parameters of the feedback-error-learning approach

Parameters	**Values**
K_p, K_i, K_d	$[0.5 \quad 0 \quad 0.9]$
L_{input}	70
L_{hidden}	200
η_{input}	0.000045
η_{hidden}	0.000015
M	1

These parameters were adjusted using an empirical approach, which took in consideration the properties and the stability of the system, such as the time of convergence of the neural network and the hardware/software used in the experimental setup. A sampling period of 0.1 second was used during the experiment.

A sine signal was used as the reference *ref* with a period of 8 seconds and amplitude equivalent to a rotational movement of $\pm 20^{o}$. To compare both control approaches, this reference and the same feedback gains were also used for the case when just the *PID* controller was employed.

During training a period of the sine reference signal was presented 85 times. The neural network took around 200 seconds to converge to a solution. After convergence, the output of the system closely followed the input reference signal.

Figure 3 shows the reference and output signal for both cases: *PID* and *PID+NN* at the end of the training session. The performance of the *feedback-error-learning* is increased if one puts a smaller learning rate while keeping the training phase longer. Using this procedure the feedback-error-learning strategy was able to track the reference signal closer than the *PID* controller.

Figure 4 shows the output of the tachometer for the *PID* and the *PID+NN* controller at the end of the training session. The tachometer signal for the *PID+NN* presents less harmonic content than the case of the *PID*. The *PID+NN* resembles better a sine wave and also seems to better adapt to the flexible system nonlinearities.

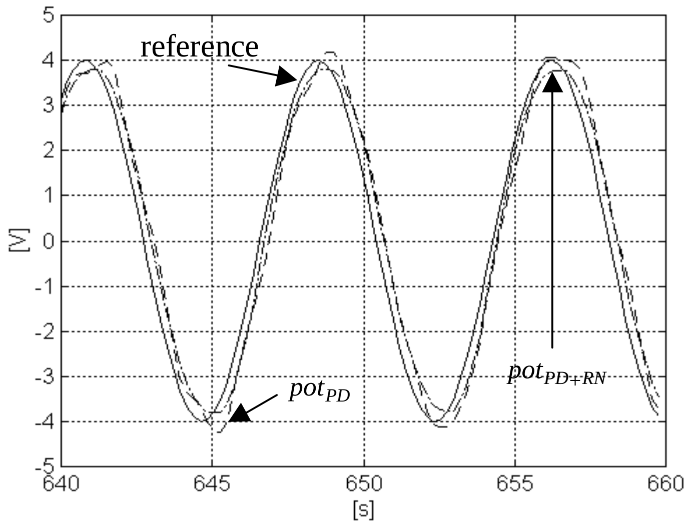

Figure 3- Comparison of the potentiometer and reference signal for both case: *PID* and *PID+NN*

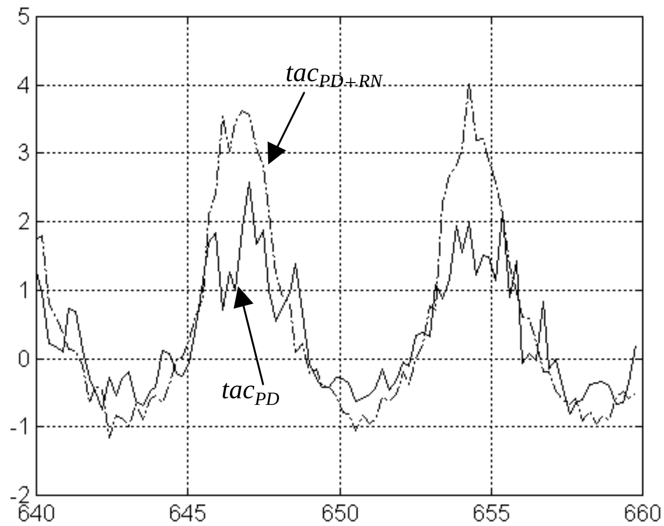

Figure 4- Comparison of the tachometer signal for both case: *PID* and *PID+NN*

Figure 5 shows the quadratic mean values of the error signal E (input of the feedback controller) and U_{FB} (output of the feedback controller) for the case *PID*. Figure 6 shows the quadratic mean values of the error signal E, U_{FB}, U_{NN} (output of the neural network), U (control signal, $U = U_{FB} + U_{NN}$) for the case *PID+NN*. The quadratic mean values were calculated for each period of the reference signal.

Figure 6 shows that at the end of the training session, the neural network output U_{NN} is the dominant part of the control signal U. This means that the neural network is a good delayed inverse model of the system, at least for the reference signal that was used during training.

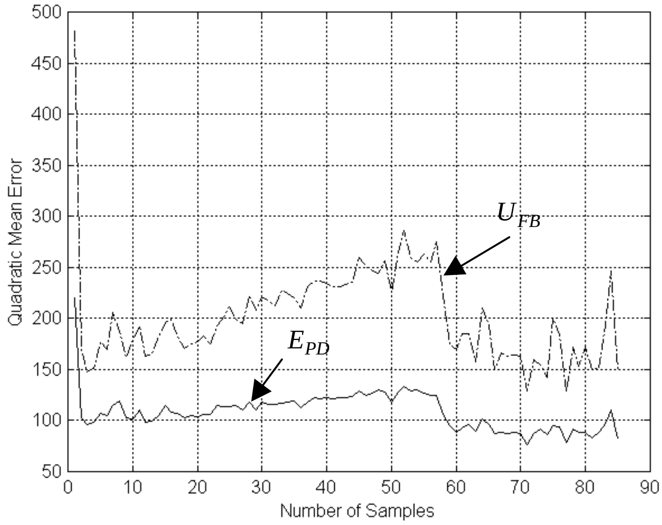

Figure 5- Quadratic mean values of E and U_{FB} for the case *PID* control

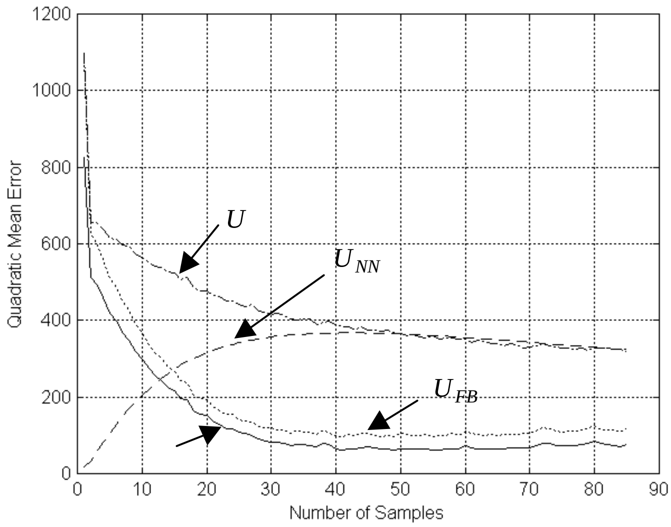

Figure 6- Quadratic mean values of E, U_{FB} , U_{NN}, and U for the case *PID+NN* control

5. CONCLUSIONS

This paper shows the implementation of an experimental neural control strategy of an unconstrained nonlinear multibody system with flexible appendages. The approach used was the *Feedback-Error-Learning* and the applied neural network was a nonlinear multilayer Perceptron trained with the *Back-Propagation* learning algorithm.

The nonlinear analytical model of the unconstrained multibody system was presented, where the appendage-to-hub inertia ratio is 37, which is considered a high value and makes most control approaches very sensitive to the nonlinearities of the system.

As expected, in the feedback-error-learning approach the neural network dominated the control signal after a short period of training time (Rios-Neto, 1998). This approach shows good potential for positional and active vibration control of multibody flexible systems.

This work also shows the benefits of the integration of two research areas: the control of flexible structures and the use of artificial intelligence.

REFERENCES

Barbieri, E., & Özgüner, Ü., 1988, Unconstrained and Constrained Mode Expansions for a Flexible Slewing Link. Journal of Dynamic Systems, Measurement, and Control. vol. 110, pp. 416-421.

Gildin, E., 1997, Desenvolvimento de Um Controlador Adaptativo Para Manipuladores Flexíveis Com Incertezas de Carga. (Development of an Adaptive Controller for Flexible Manipulators with Load Uncertain), Master Thesis, Universidade de São Paulo, 1997.

Góes, L. C. S., Negrão, R. G., Rios Neto, W., 1998. Modeling and Control of Multibody System with Flexible Appendages., eds Balthazar, J. M., Gonçalves, P. B. and Clayssen, J. (Editors), Nonlinear Dynamics, Chaos, Control and Their Applications to Engineering Sciences. Vol 2: Vibrations with Measurements and Control, published by Brazilian Society of Mechanical Sciences - ABCM, Brazilian Society of Computational and Applied Mathematics - SBMAC and Society for Industrial and Applied Mathematics - SIAM, pp. 75-91.

Nascimento Jr., Cairo L., 1994, Artificial Neural Networks in Control and Optimization, PhD Thesis, Control Systems Centre, UMIST, Manchester, UK.

Rios-Neto, W., 1998, Controle de um Sistema com Apêndices Flexíveis usando Redes Neurais (Control of a System with Flexible Appendages using Neural Networks), Master Thesis, Instituto Tecnológico de Aeronáutica, São José dos Campos, Brazil.

Rios-Neto, W., Nascimento Jr., C. L., Góes, L. C. S., 1998, Controle Adaptativo Inverso usando Feedback-Error-Learning (Inverse Adaptive Control using Feedback-Error-Learning), Proceedings of the 12th Brazilian Automatic Control Conference, 14-18 Sept., Uberlândia, Brazil, vol. I, pp. 351-356.